

Intermittent current interruption method for commercial lithium ion batteries aging characterization

Zeyang Geng, Torbjörn Thiringer *Senior Member, IEEE*, and Matthew J. Lacey

Abstract—In this article, a pioneering study is presented where the intermittent current interruption method is used to characterize the aging behaviour of commercial lithium ion batteries. With a very resource-efficient implementation, this method can track the battery resistive and diffusive behaviours over the entire state of charge range and be able to determine the aging throughout the life time of the batteries. In addition, the incremental capacity analysis can be carried out with the same data set. This method can provide measurement results with a high repeatability and produce equivalent information as the electrochemical impedance spectroscopy method. In this study, both the resistive and diffusive parameters increase with the battery capacity fading. This method does not require advanced test equipment and even with a 0.1 Hz sampling frequency, it is possible to extract usable parameters by prolonging the interruption length. Therefore, it has the potential to be easily implemented in the charging sequence in electric vehicles or stationary storage batteries for aging diagnostics.

Index Terms—Aging, Batteries, Measurement

I. INTRODUCTION

To fulfill the battery warranty to the customers, the manufacturers of electric vehicles need to predict the lifetime of their lithium ion batteries depending on the assumed usage. Despite the high cost, a massive accelerated aging test performed in a laboratory environment is still the required approach to estimate the battery lifetime [1], [2], [3]. During the lifetime testing, a reference performance test (RPT) needs to be performed regularly to track the battery performance [4]. An RPT often consists a series of characterization tests to obtain the important performance properties, such as capacity and resistance [5], [6]. Although there are international standards that suggest test specifications for commercial batteries [7], [8], [9], there is no standard RPT procedure and instead it is designed and adapted depending on the purpose and available facility.

The most common test methods used in RPTs are the capacity test and pulse test [10], [11], [12]. The capacity test

includes constant current constant voltage (CCCV) capacity test and constant current (CC) discharge capacity test. The CCCV capacity test quantifies the thermodynamic capacity of the cell and the CC discharge capacity test evaluate the usable capacity under a certain C-rate. The pulse test can be designed as different variants from the standard hybrid pulse power characterization (HPPC) test [13]. The result from a base pulse test is an overall internal impedance, contributed from the complex electrochemical processes, at a certain C-rate and time length [14]. Both the capacity test and pulse test are simple and easy to implement in an RPT procedure, but can only provide basic indicators for the battery SOH. There are other advanced characterization methods that are possible to be employed in an RPT to track more detailed aging properties, including the galvanostatic intermittent titration technique (GITT) and electrochemical impedance spectroscopy (EIS). With a sufficient long relaxation period after each current pulse, GITT can measure the open circuit voltage (OCV) of the cell including the hysteresis [15]. However, to achieve an accurate result, the relaxation period should be at least one hour [16] and can be up to four hours [17]. The long test period introduces extra calendar aging during the lifetime test making GITT less popular in RPTs. Besides the OCV, this technique can also be used to measure the diffusion coefficient of electrode materials [18], [19], [20]. Compared with GITT, EIS can not only provide information about the diffusion process, which is pronounced in the low frequency range, but also the kinetic properties and ohmic resistance [21]. Despite the challenges in interpreting the results, EIS is a very powerful tool for aging characterization [22], [23]. However, performing an EIS requires dedicated hardware and is thus beyond the capability of most of the testers used in a massive lifetime test. Therefore, either only a limited number of cells can be characterized with the EIS technique during aging, or the cells under test need to be manually reconnected to a different instrument to perform EIS. The re-connections will disturb the test, causing experiment errors [24] and requiring extra time and effort.

Among the available test methods used in RPTs for commercial batteries, the capacity test and pulse test are practical but only provide basic aging information. GITT takes a long test time which can cause extra aging, and EIS requires a special instrument. Therefore, it is of great interest to introduce an effective characterization method which can track the battery aging behaviors in detail and can be performed with regular battery testers or even with ordinary battery charging systems.

Z. Geng and T. Thiringer are with the Department of Electrical Engineering, Division of Electric Power Engineering, Chalmers University of Technology, 412 96 Gothenburg, Sweden (e-mail: zeyang.geng@chalmers.se, torbjorn.thiringer@chalmers.se).

Matthew J. Lacey is with Scania CV AB, 15187 Södertälje, Sweden (e-mail: matthew.lacey@scania.com)

This paper has been accepted for publication by IEEE. DOI (identifier) 10.1109/TTE.2021.3125418. © Copyright 2021 IEEE. Personal use of this material is permitted. Permission from IEEE must be obtained for all other uses, in any current or future media, including reprinting/republishing this material for advertising or promotional purposes, creating new collective works, for resale or redistribution to servers or lists, or reuse of any copyrighted component of this work in other works.

In [25], a new intermittent current interruption (ICI) test was used to measure the resistance values for lithium sulfur batteries. This concept has also been employed for lithium ion [26], [27], [28] and sodium ion [29] battery materials. Later in [30], the ICI method was extended to capture the diffusion process in lithium sulfur batteries besides the resistance values. However, in available literature, this method has only been applied on lab scaled cells, and the validation of this method for commercial cells, has not yet been performed. Moreover, the method presented in this article, in addition, has the potential to provide more information, such as incremental capacity analysis (ICA), as well as differential voltage analysis (DVA), which has not been shown previously. Furthermore, there is a need to investigate its repeatability, reliability, robustness to noise and hardware requirements, to examine the potential of this method in broader application scenarios.

The specific contribution with this article is that it closes this research gap, i.e. it demonstrates how the ICI method can be used in an RPT for commercial batteries aging characterization, in a very resource effective way. This is achieved by having the following goals: 1) The demonstration of the effectiveness of the ICI method in determining and tracking a series of properties during the course of the battery aging, including the resistive and diffusion related behaviours, as well as the incremental capacity analysis. 2) The validation that the information obtained from the ICI method and the EIS test provide fully comparable results through the battery lifetime. 3) The quantification of the extra aging effect that is caused by the RPT by having a cell running RPTs continuously. 4) The proof that a high-performance test equipment is not needed, and thus the ICI method can be implemented with basic battery testers or on-board equipment in electrified vehicles or stationary storage applications, for battery system aging diagnostics.

II. METHOD DESCRIPTION

The intermittent current interruption (ICI) method was proposed to monitor the battery status for photovoltaic systems [31] and then applied for lithium sulfur battery characterization [25]. In this method, a low current rate is applied to charge and discharge the battery and the current is interrupted with short pulses after long intervals. In this way it can be said that the current pattern in an ICI method is reversed from the current in a GITT method. One example of an ICI test is shown in the figure below where the current is interrupted for 10 s every 5 mins during a C/5 charging event.

After the current is interrupted during charging, the voltage drops quickly during the first second, and then decreases with a linear relationship with the square root of the time, as shown in Fig. 2. The voltage responses with different time constants can be related with different electrochemical processes taking place in a battery system. A commercial battery system has an inductive behaviour at a very high frequency (kHz) which is rarely captured in a pulse measurement at $t = 0$ s. At $t = 2$ ms, an instantaneous voltage drop ΔV_{2ms} can be observed which is related with the ionic resistance of the bulk electrolyte (due to the migration and not the diffusion process), as well

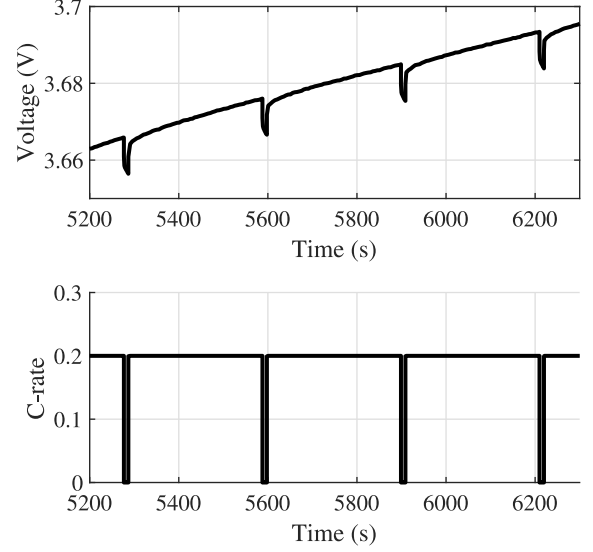


Fig. 1: An example of the ICI method implementation, where a C/5 charging current is interrupted for 10 s every 5 mins.

as the electronic resistance of the electrodes and the current collectors. With time passing, the charge transfer reactions appear in the voltage response ΔV_{1s} at $t = 1$ s. Based on the voltage change, the resistive parameters R_{2ms} and R_{1s} can be calculated as

$$R_{2ms} = -\frac{\Delta V_{2ms}}{I}, \quad (1)$$

$$R_{1s} = -\frac{\Delta V_{1s}}{I}, \quad (2)$$

where I is the current before the interruption. For a battery tester that has a moderate sampling frequency, it is more practical to capture the total voltage change ΔV_{1s} at $t = 1$ s.

The charge transfer reaction can be described with the Butler–Volmer equation

$$j = j_0 \left(\exp \frac{\alpha_a F \eta}{RT} - \exp \frac{-\alpha_c F \eta}{RT} \right) \quad (3)$$

and the charge transfer resistance at the particle surface R'_{ct} is

$$R'_{ct} = \frac{\eta}{j} \quad (4)$$

where j is the charge transfer current density per surface area, j_0 is the exchange current density, α_a and α_c are the anodic and cathodic constant, F is the Faraday constant, R is the gas constant, T is temperature and η is the overpotential caused by the redox reaction. In (4), the unit of R'_{ct} is $[\Omega \cdot \text{m}^2]$ and the area here is the total surface area of the particles. In commercial lithium ion batteries, the electrode material has a porous structure to increase the contact surface area between the particle and the electrolyte. The charge transfer resistance of the electrode R_{ct} is

$$R_{ct} = \frac{R'_{ct}}{AdS_a} \quad (5)$$

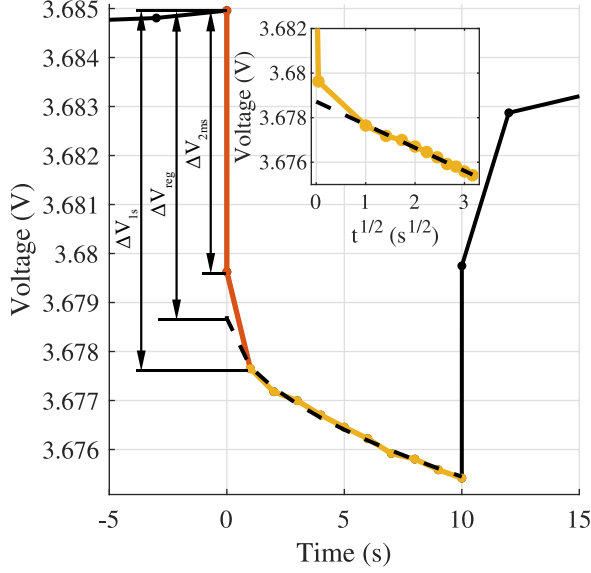


Fig. 2: The voltage response at different time constants after the current is interrupted during charging.

where A is the electrode area, d is the electrode thickness and S_a is the specific surface area, which is the total surface area per volume. In a physical model of the lithium ion battery, R_{ct} is connected with the double layer capacitor in parallel, and this RC link dynamic behaviour dominates the voltage response between 0 s and 1 s.

After 1 s, the voltage response is governed by the diffusion process in the solid as it is the slowest process, and this is similar in a GITT test. The diffusion process in the solid can be described with Fick's laws of diffusion in a spherical coordinate system

$$\frac{\partial c_s}{\partial t} = D_s \left(\frac{\partial^2 c_s}{\partial r^2} + \frac{2}{r} \frac{\partial c_s}{\partial r} \right) \quad (6)$$

where t is time, r is the distance from the particle center, c_s is the lithium ion concentration in the solid and D_s is the diffusion coefficient. The boundary condition is

$$\frac{\partial c_s}{\partial r} \Big|_{r=r_s} = -j / (F D_s) \quad (7)$$

where r_s is the particle radius, j is the current density at the particle surface and F is the Faraday constant. The symmetry of the particle also gives

$$\frac{\partial c_s}{\partial r} \Big|_{r=0} = 0 \quad (8)$$

When the current is interrupted, the voltage response V follows a linear relationship of \sqrt{t}

$$V = V_0 + \frac{dE}{dc} \frac{j}{F} \sqrt{\frac{t}{D_s}}, \quad t \ll \frac{r_s^2}{D_s} \quad (9)$$

A diffusion related parameter k can be extracted

$$k = -\frac{1}{I} \frac{dV}{dt^{1/2}}, \quad t > 1s. \quad (10)$$

In (9) the diffusion coefficient D_s is a parameter for a specific electrode material. However when measuring a commercial battery cell, it is not possible to distinguish the impact of the positive electrode and the negative electrode. Therefore the parameter k reflects the diffusion behaviour of the two electrodes.

The k value obtained from the ICI method can be correlated with the diffusion parameter σ extracted from the Warburg impedance $Z_w = \sigma \omega^{-1/2} - j \sigma \omega^{-1/2}$ in an EIS measurement, where $\omega = 2\pi f$ is the angular frequency. The relationship between σ and k has been theoretically derived in [30], where it was found to be

$$k = \sigma \sqrt{\frac{8}{\pi}}. \quad (11)$$

The time constants for different electrochemical processes depend on the materials in the battery. The 2 ms and 1 s above were selected arbitrarily based on the priori knowledge from the impedance spectrum of the battery used in this work. To remove the arbitrariness of the timescale, a linear regression analysis can be carried out, which was proposed in [25]. If the linear regression of the voltage response is backwards extrapolated to $t = 0$, a voltage change ΔV_{reg} can be calculated as shown in Fig. 2. The corresponding resistance is

$$R_{reg} = -\frac{\Delta V_{reg}}{I}. \quad (12)$$

This value R_{reg} can be accurately obtained even when the test is performed in a noisy environment or with a poor sampling rate. Therefore this parameter can be used to track the battery aging characters in field diagnostic tests. Moreover, by tracking R_{reg} instead of the resistance at a specific time, the impact of various timescales can be eliminated.

Beside the resistive and diffusive parameters, the ICA and DVA can be performed at the same time. The outcome of the ICA is a useful description of the battery aging status [32].

The results from the ICI method can be affected by the current magnitude. With a lower current, the battery is closer to the equilibrium state during the test, providing more detailed ICA and DVA curves, but on the other hand, this unfortunately leads to a longer test time. With a higher current, the charge transfer resistance in (4) decreases and the diffusion parameter k is also affected by the concentration polarization built up in the electrolyte. The C/5 current rate selected in this work is a trade off between testing time and validity of the extracted information.

III. EXPERIMENT RESULTS AND ANALYSIS

In this section, the method's repeatability is verified first and then the ICI method is included in the RPT sequence during a lifetime test to demonstrate how the ICI method can be used to track the battery aging phenomenon. During the lifetime, an EIS is performed after each ICI to show the correlation between the two methods. In parallel, a cell has been cycled with the RPT sequence only to evaluate the aging effect introduced by the RPT.

The test objects used in this work are 26 Ah lithium ion pouch cells with a voltage window of 2.8 V - 4.15 V. The

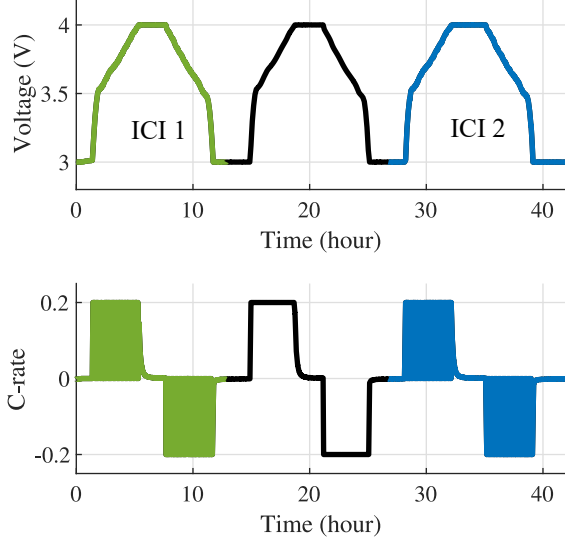


Fig. 3: Two ICI tests are performed with a regular CCCV cycle in between to examine the repeatability of the method. Zoom-in details are shown in Fig. 1 and Fig. 2.

positive electrode is a mixture of $\text{LiNi}_{0.33}\text{Mn}_{0.33}\text{Co}_{0.33}\text{O}_2$ and LiMn_2O_4 and the negative electrode is graphite. During the test, the cells are placed in a test jig with a certain pressure applied. All the tests are performed in a temperature chamber set at 25 °C. The cycling equipment is a PEC ACT0550.

A. Repeatability of the ICI method

In Fig. 3, a test procedure is implemented to verify the repeatability of the measurement result obtained from the ICI method, where a regular CCCV cycle is applied in between two ICI tests. The zoom-in details are shown in Fig. 1 and Fig. 2. The results obtained from the two ICI tests are presented in Fig. 4 and Fig. 5. The excellent repeatability of the experimental result shows that the method can be used to characterize the battery aging with a high reliability.

It can be observed in Fig. 4 that the pure resistive parameter R_{2ms} is independent from the state of charge (SOC) since the ionic resistance of the bulk electrolyte and the electronic resistance of the electrodes and current collector are not affected by the SOC. On the other hand, R_{reg} and R_{1s} show a clear increasing trend towards the low SOC range. The diffusion related parameter k is higher at the low SOC, indicating a decreased diffusion coefficient. Moreover, the k value has a distinct peak around 70 % SOC. In both the resistive parameter R_{reg} and R_{1s} and the diffusive parameter k , a slight difference can be observed in the parameter values obtained during the charging process and discharging process.

Fig. 5 shows the ICA plot of the battery. The peaks in the ICA plot correspond to the plateaus in the voltage profile, which are signs of the phase changes in the electrode materials. As can be noted from the figure, the ICA plot obtained from the ICI data agrees very well with the plot obtained from a

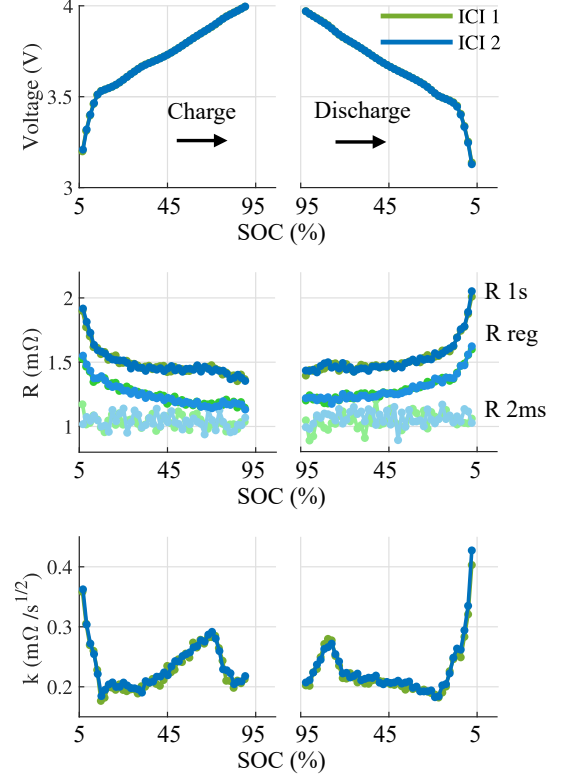


Fig. 4: The parameters R_{2ms} , R_{reg} , R_{1s} and k obtained from the two ICI tests in Fig. 3 showing a high repeatability.

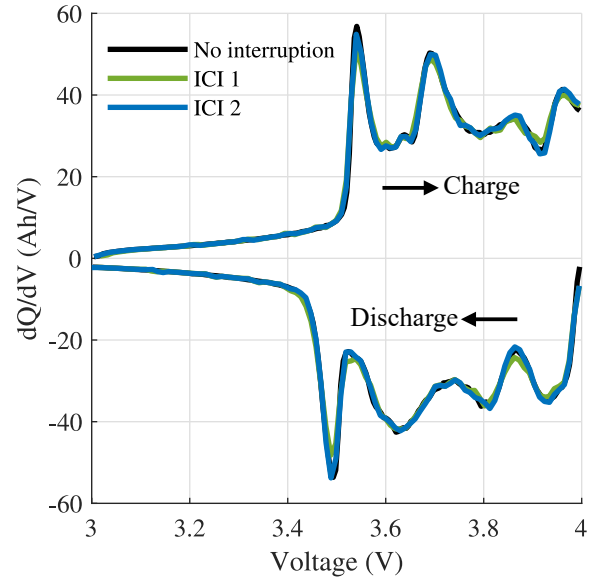


Fig. 5: The incremental capacity analysis based on the two ICI tests in Fig. 3 and a regular CCCV cycle without current interruption.

regular CCCV cycle. This shows that the current interruptions in the ICI method does not introduce significant artefacts in the analysis.

B. Tests at different temperatures

Lithium-ion batteries can operate over a wide temperature range and its electrical properties are highly dependent on the temperature. In this section, the validity of the ICI method at different temperatures are investigated. The temperature condition of the test is from -20°C to 40°C , with a step of 10°C , and it covers most of the temperature operation conditions for batteries in electric vehicles. The battery cell under test is located in an ESPEC LU-124 climate chamber. Before each test, the battery is left in the desired ambient temperature for at least 8 hours to allow it to reach a thermal equilibrium state and the cell is CCCV discharged to its minimum SOC. The test procedure is a 10 s pulse every 5 mins during a C/5 charge and discharge, the same in all temperature conditions. The test results are shown in Fig. 6. The figures on the left present the data over the entire SOC range at different temperatures and the color coding is according to the figures on the right. The y-axis in the three figures on the left are in logarithmic scale to provide a clear visualization. From the test at each temperature, the electrical properties, R_{2ms} , R_{reg} and k measured at 3.8 V during discharge are selected and plotted versus the temperature in the figures on the right, with a linear scale on the y-axis. There is an underestimation of the R_{reg} values when the SOC is lower than 10 %, at the very low temperature conditions, i.e. -20°C and -10°C , where the voltage response is not diffusion controlled anymore during the interruptions. It can be seen that at a lower temperature, both the resistive parameters R_{2ms} and R_{reg} and the diffusive parameter k are higher. This is because the electrolyte conductivity, exchange current density and diffusion coefficients (both in the particle and in the electrolyte) decrease at lower temperature, resulting in higher resistance values. This trend appear at the entire SOC range, both during charge and discharge. The test results show that the ICI method can be applied at different temperatures to characterize batteries without adjusting the design of the test. Despite the fact that the time constant of charge transfer reaction varies at different temperature, the linear regression approach removes the arbitrariness of the timescale, and one can obtain essentially time-independent quantities to describe the resistance of the system.

C. Aging test

During the aging test, the battery cell has been cycled with +2C/-2C constant current in a voltage window of 3 V - 4 V at 25°C . An RPT is scheduled regularly to track the battery performance. The RPT sequence is shown in Fig. 7, including a 1C capacity test, ICI test, 1 kHz AC impedance test, EIS test and pulse tests. The 1C capacity is measured between 3 V and 4 V and the ICI test is implemented with C/5 current and 5 s interruption every 5 mins. A sequence of 1 kHz AC impedance test and EIS test is performed at 2.8 V, 3.7 V and 4.15 V respectively. 2 C charge pulse tests are performed at

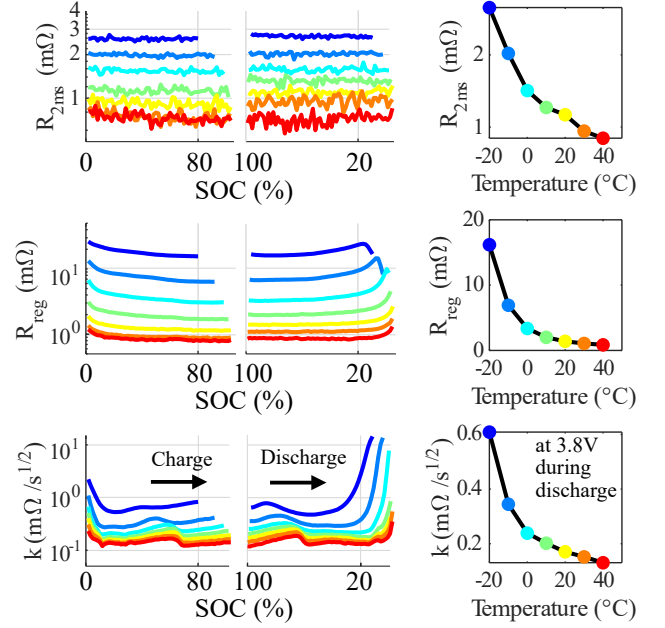


Fig. 6: Results of ICI tests performed at different temperatures from -20°C to 40°C .

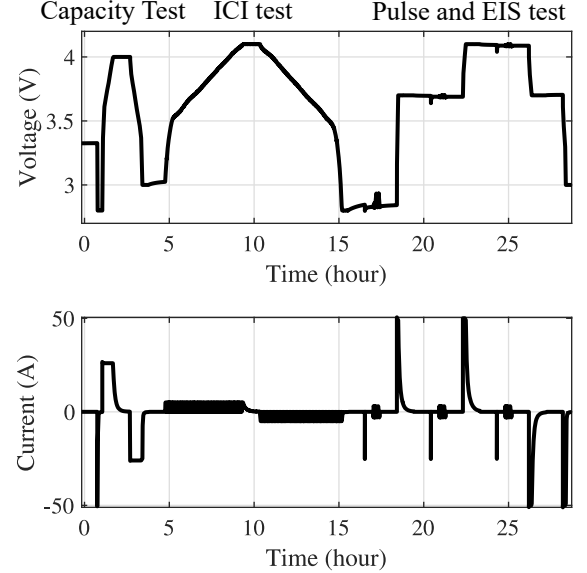


Fig. 7: The RPT sequence used in the aging test, including a 1C capacity test, ICI test, 1 kHz AC impedance test, EIS test and pulse tests.

2.8 V and 3.7 V, and 2 C discharge pulse tests are performed at 4.15 V and 3.7 V.

The tester used in the aging test does not have a built-in EIS function, and therefore a current pattern consisting sinusoidal waves with different frequencies is generated in MATLAB and implemented as a drive cycle in the tester. The highest update rate and sampling rate of the input current is 1 kHz and the maximum frequency of a sine wave that can be generated without too much distortion is thus approximately 100 Hz.

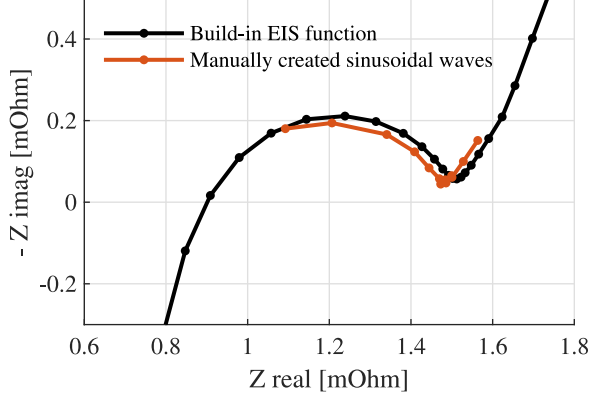


Fig. 8: Verification of the EIS result obtained with a manually created sine waves pattern.

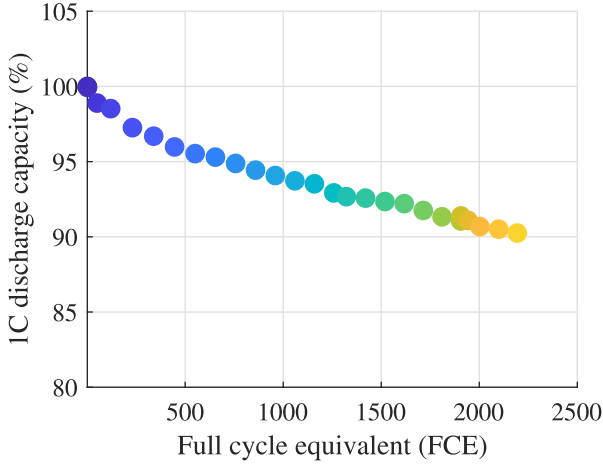


Fig. 9: The degradation of the 1C discharge capacity of the investigated cell.

This approach has been verified with a potentiostat GAMRY Reference 3000 which is dedicated for EIS measurement. The impedance result measured with the GAMRY built-in EIS function and with the manually generated sine waves are compared in Fig. 8. It shows that the manually created sine wave pattern can be used to extract the impedance information and it can provide a trustworthy result within a limited frequency range. This method can be applied in general to obtain an EIS plot within a limited frequency range even the battery tester that does not have a built-in EIS functionality. Another alternative is to use a pseudo-random binary sequences (PRBS) which has been proved in [33].

The degradation of the cell 1C discharge capacity is shown in Fig. 9 and each dot represent one RPT. The 1C discharge capacity at the beginning of life (BOL) is set as 100 % and it has only decreased to 90 % after 2000 full cycle equivalent (FCE). The cell used in this work is a commercial cell for electric vehicle application and it has an excellent performance as well as lifetime.

From the ICI tests in the RPT, the extracted properties are presented in Fig. 10 and Fig. 13. The pure resistive parameter

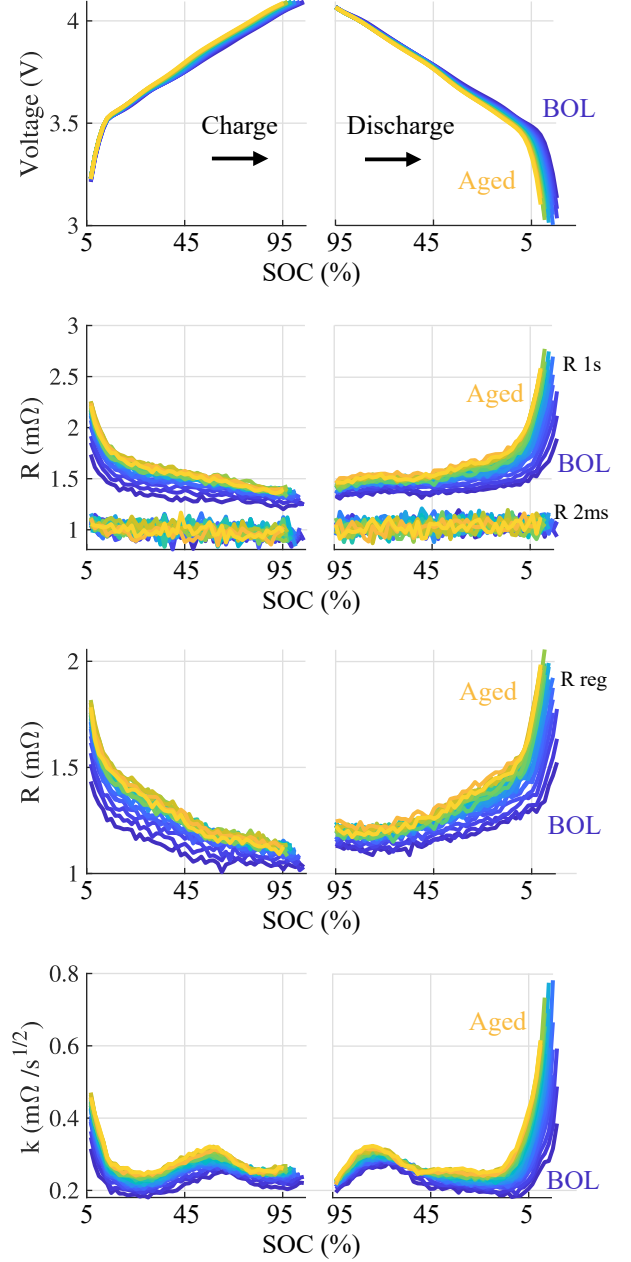


Fig. 10: The resistive and diffusive parameters obtained from the ICI method during the battery aging.

R_{2ms} remains at the same level through the battery lifetime, implying that there is little degradation in the electrolyte which results in any notable change in electrolyte resistance, and no significant corrosion in the current collectors. On the other hand, there are significant increases in both R_{reg} and

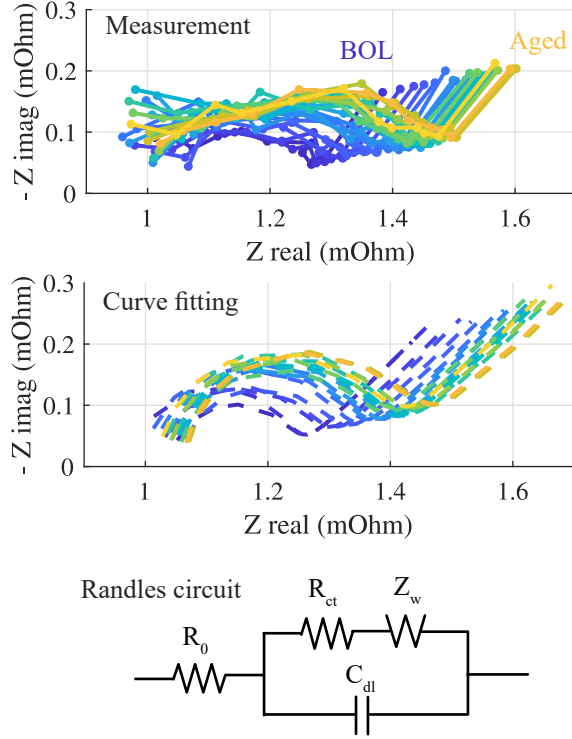


Fig. 11: The cell impedance (100 Hz - 50 mHz) at 3.7 V increases with aging.

R_{1s} for the entire SOC range. These two parameters include the pure resistive component, as well as the charge transfer resistance and the solid electrolyte interphase (SEI) resistance. Since R_{2ms} shows a constant behaviour, it indicates that the increases in R_{reg} and R_{1s} are possibly due to changes taking place at the electrodes, with a major contributor expected to be the growth of the SEI layer at the negative electrode as is typically observed for lithium-ion batteries [2]. Similarly, the diffusion parameter k rises with the cell degrading, meaning a slower diffusion process for an aged battery. This can also be resulted by an increased SEI layer and a lower specific surface area. It can be observed that the parameter increases are more pronounced at the lower SOC range, although the very low SOC range has not been utilized during the cycling aging.

As mentioned in (11), the ICI method can provide similar diagnostic information as the EIS method. In this aging test, the battery impedance between 100 Hz and 50 mHz is measured with a series of sinusoidal current waves as the input at different voltage levels. The impedance measurements are fitted with the Randles circuit, where R_0 represents the sum of the electronic and ionic resistances, R_{ct} stands for the charge transfer resistance, C_{dl} is the double layer capacitance and $Z_w = \sigma\omega^{-1/2} - j\sigma\omega^{-1/2}$ is the Warburg impedance resulting from the diffusion processes. The diffusion parameter σ can be extracted from the Warburg impedance and then be translated to k according to (4).

In Fig. 11, the impedance increase at 3.7 V resulting from the cycling aging, as well as the curve fittings, are presented. $R_0 + R_{ct}$ and k extracted from the EIS measurement at 3.7

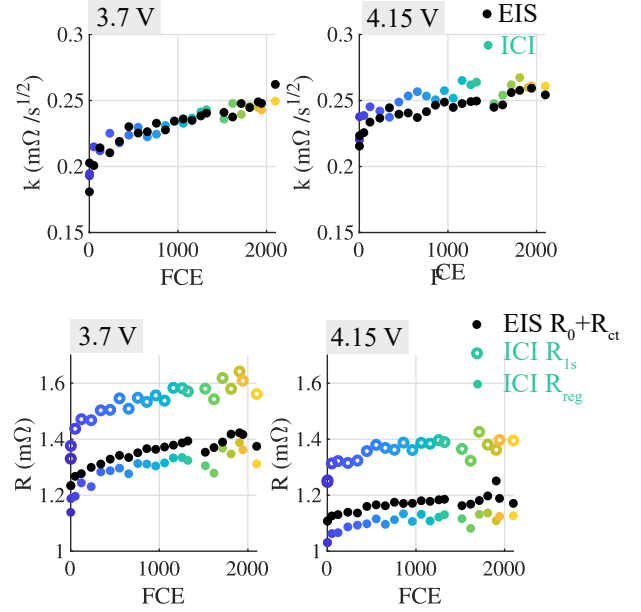


Fig. 12: A comparison of the parameters obtained from the ICI method and EIS method.

V and 4.15 V are plotted in Fig. 12 (black dots), showing the expected behaviours, that both parameters increase during the cycling aging. In the same plot, the parameters R_{reg} , R_{1s} , and k obtained from the ICI method, are compared at two voltage levels. There is a very good agreement in the k values obtained from the EIS and ICI method during the entire lifetime test at both voltage levels. Meanwhile, the EIS parameter $R_0 + R_{ct}$ values match with the ICI parameter R_{reg} . Although the extracted parameters contain mixed information from the two electrodes, they are related to the actual physical processes and thus are useful indicators for the degradation phenomena. Fig. 12 shows that the ICI method can provide equivalent information as the EIS method regarding the resistance and diffusion parameters and the ICI can provide this information over the entire SOC range as demonstrated in Fig. 10.

Besides tracking the resistance and diffusion parameters, the ICI method can provide data for the incremental capacity plot in Fig. 13 and the differential voltage analysis in Fig. 14, which reveal where the capacity loss occurs. A decreased peak in Fig. 13 is indicating a reduced capacity at the corresponding phase.

D. Aging effect introduced by RPTs

It is important to evaluate and limit the extra aging introduced by the RPT sequence so that the RPT itself does not influence the cycling aging considerably. In this work, a cell of the same type used in the previous aging test has been cycled continuously with the RPT in Fig. 7 and the degradation of its 1C discharge capacity is shown in Fig. 15. After 400 repetitive RPTs, the battery lost 8 % of the capacity meaning that each RPT will roughly age the battery 0.02 %. In Fig. 9, 27 RPTs have been performed for diagnostics over 2200 FCEs, which in total can cause around 0.54 % capacity loss. Compared with

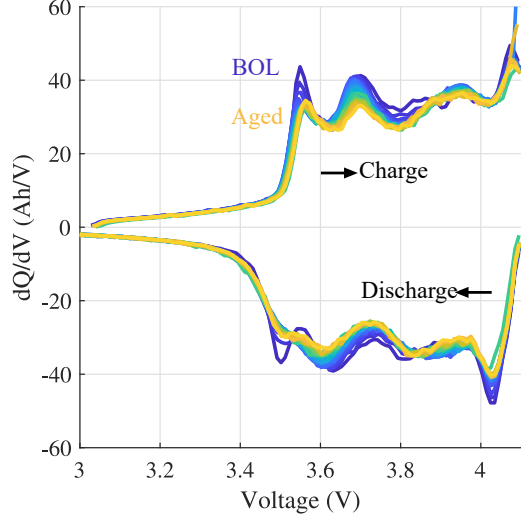


Fig. 13: The incremental capacity analysis with the ICI data to track the battery degradation.

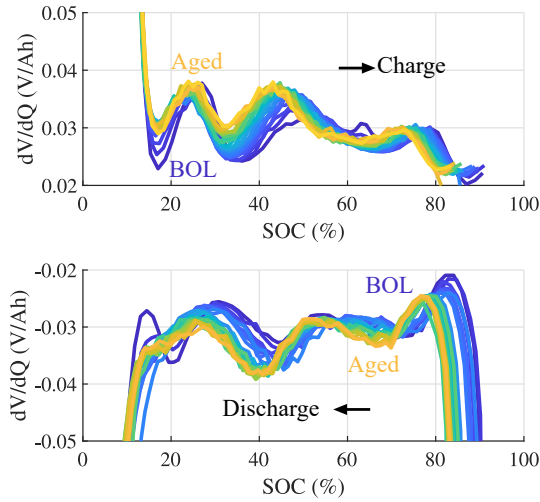


Fig. 14: The differential voltage analysis with the ICI data.

the 10 % capacity loss during the cycling aging, the diagnostic tests introduces around 5% extra aging, which is acceptable. This effect can be reduced further if the RPT is performed less frequent and with a simplified procedure. As shown in this article, it is possible to include only the 1 C capacity and the ICI test in the RPT, since the two tests can provide sufficient information for aging analysis.

E. Analysis of the implementation requirements

In the previous sections, it has been proved that the ICI method is able to provide high quality results with measurements obtained from an advanced battery tester (max 1 kHz sampling frequency and the voltage measurement accuracy is within ± 0.005 % full scale deviation) in a controlled lab environment. However, as indicated in the introduction of this

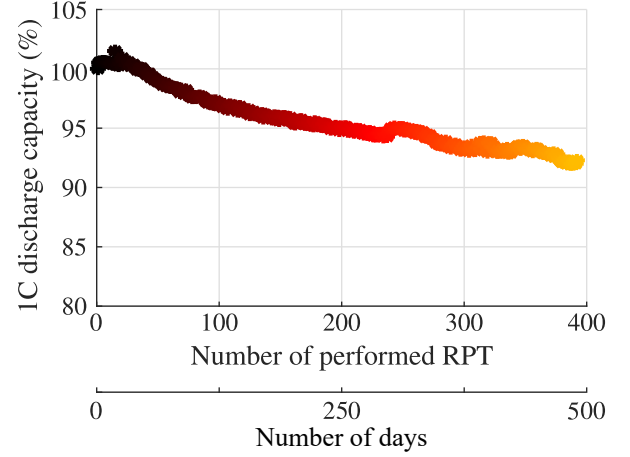


Fig. 15: The cell capacity degradation with RPTs performed continuously.

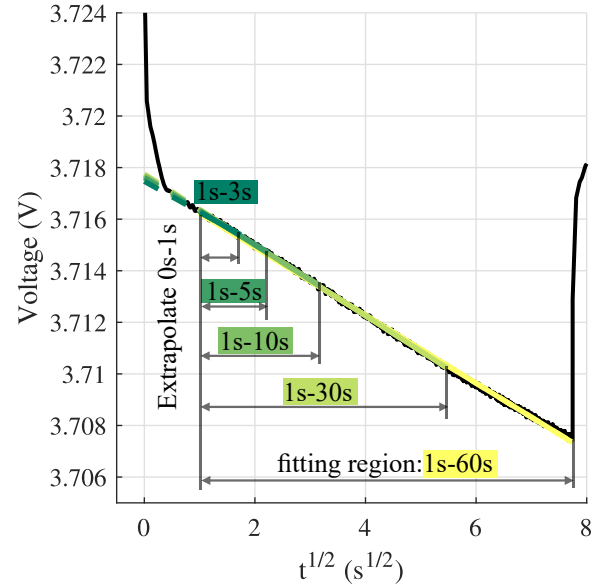


Fig. 16: Different interruption lengths are used to extract the R_{reg} and k parameters.

article, the ICI method does not require high performance equipment and it can be applied with a normal tester or on-board equipment in an ordinary battery system.

In Fig. 1 and Fig. 2, the interruption length was 10 s and the sampling frequency was 1 Hz (one extra sample at 2 ms after the current interruption) and the corresponding results in Fig. 4 and Fig. 5 showed the battery properties with clear trends. In many applications, including electric vehicles, 1 Hz or a higher sampling frequency is available, therefore the procedure described previously can be directly adapted in a charging event. However, in some other applications, for example in a stationary storage, the data acquisition system might not be able to log the data fast enough. In such cases, a longer interruption period can be adapted to extract the resistance R_{reg} in (5) and a diffusion related k parameter in (4). In

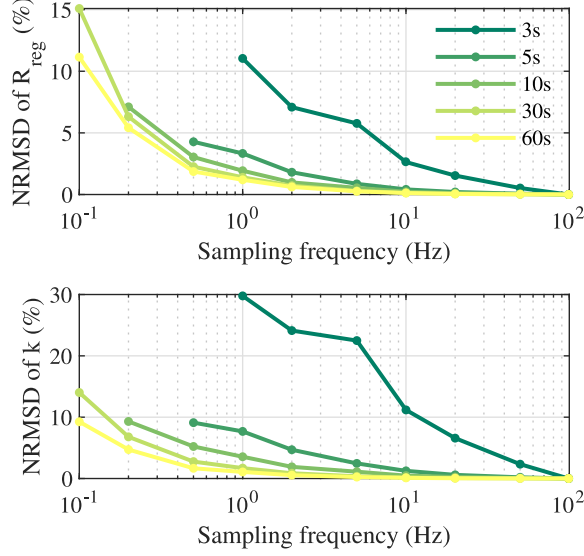


Fig. 17: Normalized root mean square deviations (NRMSDs) of the results extracted with different sampling frequencies for each interruption length case.

Fig. 16, the voltage response during a 60 s current interruption during charging is plotted versus $t^{1/2}$. For each interruption length, the result obtained from the original measurement (500 Hz sampling) is considered as the reference result. The deviations of the results obtained from a down-sampled data are shown in Fig. 17 (only during charging). The normalized root mean square deviation (NRMSD) is calculated as

$$RMSE(f_s) = \sqrt{\frac{\sum_{i=1}^N (x_{i,f_s} - x_{i,500Hz})^2}{N}}, \quad (13)$$

$$NRMSD(f_s) = \frac{RMSE(f_s)}{x_{avg}}, \quad (14)$$

where x_i is the R_{reg} or k at each SOC level and f_s is the used sampling frequency. It can be observed that if the system is capable of sampling faster than 1 Hz, a 5 s interruption length is sufficient to obtain data with less than 5% NRMSD. With a slower data acquisition system, for example 0.1 Hz, a result with around 10 % NRMSD can be achieved by prolonging the interruption length to 60 s.

In Fig. 17, the results with 500 Hz in each interruption length case are used as the reference. However, the interruption length itself will introduce deviations in the results, as shown in Fig. 18. It shows that a longer interruption length will lead to an overestimation in the R_{reg} values and an underestimation in the k values. This impact is more significant at the lower SOC ranges.

Not only is the sampling frequency the limitation factor of the equipment in the applications, but also the sensor accuracy, resolution and the noise level in the environment. In the investigation, the measurement is down-sampled to 1 Hz first, and then in one case a Gaussian noise is added with 80 dB signal to noise ratio (SNR), while in the other case, the

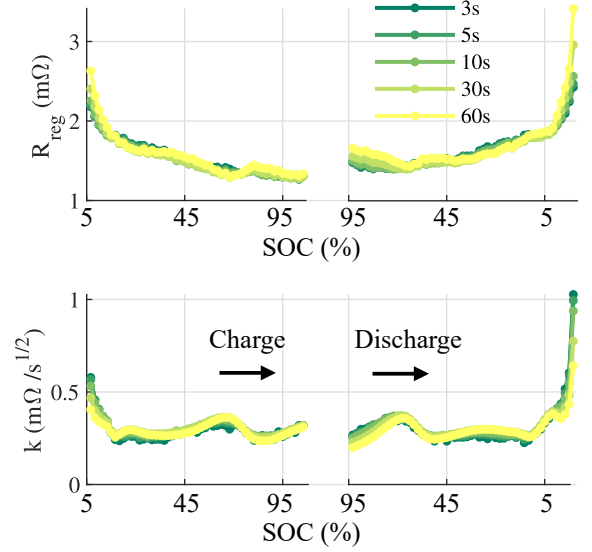


Fig. 18: R_{reg} and k values obtained with different interruption lengths with 500 Hz sampling frequency.

resolution of the voltage measured is reduced to 1 mV with a 2 mV offset. The results in Fig. 19 show that the ICI method can be utilized with sensors with a lower resolution and can tolerate a certain level of noise.

This is a promising sign that the ICI method can be implemented with on-board sensors in battery systems for aging diagnostics, besides being used in laboratory tests. One example is to implement the ICI method in an electric vehicle during selected charging events. The hardware and software implementation are similar as for the pulse charging strategy, demonstrated in [34], [35]. A difference towards the pulse charging, which can be used with both fast charging and slow charging infrastructures, is that the ICI method is more suitable to use with slow charging to provide clear diagnostic information (R_{reg} , k , ICA and DVA curves). In principle, each time the vehicle is connected to a slow charger (most likely at home during the night), and the SOC is below a certain threshold, the user could choose to perform the ICI diagnostic during charging. Today BEVs have a battery pack ranging from 20 kWh to 100 kWh. On-board chargers utilising standard power outlets have a limited capacity, in Europe 3.7 kW (16 A single-phase 230 V AC), in USA up to 6 kW [36], meaning that a charging rate slower than C/5 is common. One factor favouring home charging is the price [37], where the fast charging price leads to a driving cost similar to ICE vehicles whereas home charging is 1/3 or 1/4 of that. Furthermore, an indicator towards that slow charging will remain is the life time of the battery. In [37], an increase of 78 % of the battery resistance was reported after 120 fast charging events. Therefore, even in countries where home charging might be less common, e.g. China, it can definitely be favourable to use slow charging for overnight and over-day (work) parking. Regardless, the driver could always indicate when the car is being connected for charging, that the car is not needed for

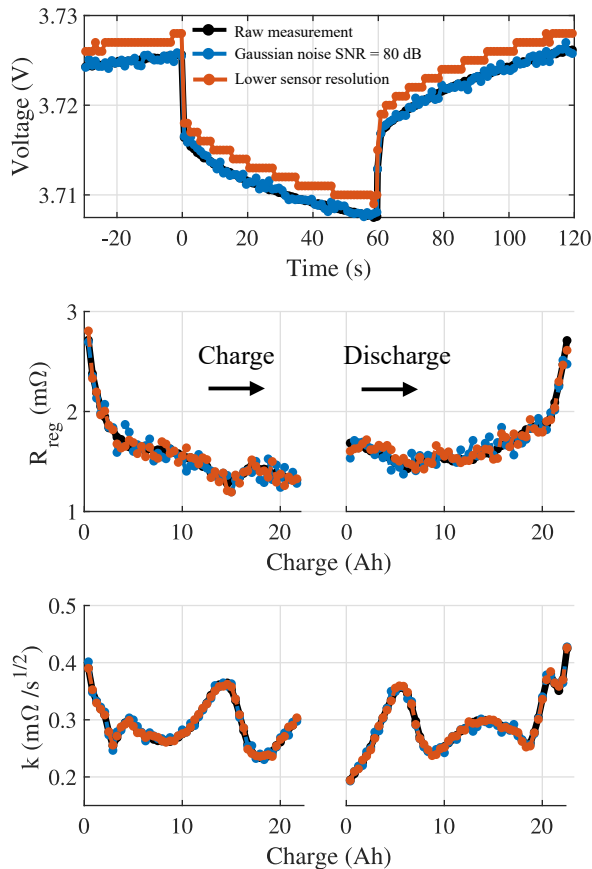


Fig. 19: How the sensor resolution and environment noise affect the ICI method results.

6 hours, and the test can be automatically conducted. When the ICI method is implemented in the charging procedure, the charging time will be less than 3 % longer (with the example of 10 s pulse every 5 mins during the constant current charge phase). Not only does it not disturb the drivers' usage, but also it can be beneficial for the battery lifetime, in a similar way as the pulse charging [38], [39].

IV. CONCLUSIONS

This work demonstrated the application of the intermittent current interruption method on commercial lithium ion batteries which has not been reported before. This method can extract most of the measurable electrical properties with a high repeatability. The parameters can be tracked during a battery life testing and have a very good correlation between the information extracted from the performed EIS measurements. It is noteworthy that the parameters R_{reg} and k from the ICI method are connected to physical processes and can therefore be used to characterise the battery degradation with different aging phenomena. The aging impact of the RPT sequence (including a capacity test, ICI test, 1 kHz AC impedance test, EIS test, charge and discharge pulse tests) is evaluated with a cell running the RPT continuously. One complete RPT can cause roughly 0.54 % loss in the 1C discharge capacity. This

impact can be reduced with a less frequent RPT schedule and a simplified RPT sequence, so the aging test can better target the specific case under investigation.

Among the parameters that can be extracted from one ICI test, R_{reg} and k rely on a linear regression of the measurement data, and therefore these two parameters can be tracked easily even in a field test with limited sensor accuracy, signal to noise ratio and sampling frequency. A very interesting possibility introduced through the results in this article is that the ICI method has been shown to have the potential to be implemented in a charging sequence in electric vehicles and stationary storage applications, to track the battery aging properties.

ACKNOWLEDGMENT

The authors would like to thank Energimyndigheten (P42789-1 and P45538-1) for the financing of this work.

REFERENCES

- [1] J. Groot, "State-of-health estimation of Li-ion batteries: Cycle life test methods," 2012.
- [2] E. Wikner et al., "Lithium ion battery aging: Battery lifetime testing and physics-based modeling for electric vehicle applications," Ph.D. dissertation, Department of Electrical Engineering, Chalmers University of Technology, 2017.
- [3] J. Wang, J. Purewal, P. Liu, J. Hicks-Garner, S. Soukazian, E. Sherman, A. Sorenson, L. Vu, H. Tataria, and M. W. Verbrugge, "Degradation of lithium ion batteries employing graphite negatives and nickel-cobalt-manganese oxide+ spinel manganese oxide positives: Part 1, aging mechanisms and life estimation," *Journal of Power Sources*, vol. 269, pp. 937–948, 2014.
- [4] M. Dubarry and G. Baure, "Perspective on commercial Li-ion battery testing, best practices for simple and effective protocols," *Electronics*, vol. 9, no. 1, p. 152, 2020.
- [5] A. Barai, K. Uddin, M. Dubarry, L. Somerville, A. McGordon, P. Jennings, and I. Bloom, "A comparison of methodologies for the non-invasive characterisation of commercial Li-ion cells," *Progress in Energy and Combustion Science*, vol. 72, pp. 1–31, 2019.
- [6] G. Mulder, N. Omar, S. Pauwels, F. Leemans, B. Verbrugge, W. De Nijs, P. Van den Bossche, D. Six, and J. Van Mierlo, "Enhanced test methods to characterise automotive battery cells," *Journal of Power Sources*, vol. 196, no. 23, pp. 10 079–10 087, 2011.
- [7] I. E. Commission et al., "Secondary lithium-ion cells for the propulsion of electric road vehicles-part 1: performance testing," *Geneva, Switzerland*, pp. 62 660–1, 2011.
- [8] I. ISO, "12405-1: 2011-electrically propelled road vehicles—test specification for lithium-ion traction battery packs and systems—part 1: High-power applications," *ISO: Geneva, Switzerland*, 2011.
- [9] B. ISO, "12405-2: 2012, electrically propelled road vehicles—test specification for lithium-ion traction battery packs and systems; part 2: Highenergy applications," *British Standards Institution*, 2012.
- [10] X. Han, M. Ouyang, L. Lu, J. Li, Y. Zheng, and Z. Li, "A comparative study of commercial lithium ion battery cycle life in electrical vehicle: Aging mechanism identification," *Journal of Power Sources*, vol. 251, pp. 38–54, 2014.
- [11] J. Kim, H. Chun, M. Kim, J. Yu, K. Kim, T. Kim, and S. Han, "Data-driven state of health estimation of li-ion batteries with rpt-reduced experimental data," *Ieee Access*, vol. 7, pp. 106 987–106 997, 2019.
- [12] A. Soto, A. Berrueta, P. Sanchis, and A. Ursúa, "Analysis of the main battery characterization techniques and experimental comparison of commercial 18650 Li-ion cells," in *2019 IEEE International Conference on Environment and Electrical Engineering and 2019 IEEE Industrial and Commercial Power Systems Europe (EEEIC/I&CPS Europe)*. IEEE, 2019, pp. 1–6.
- [13] X. Hu, S. Li, and H. Peng, "A comparative study of equivalent circuit models for Li-ion batteries," *Journal of Power Sources*, vol. 198, pp. 359–367, 2012.

- [14] M. Ecker, N. Nieto, S. Käbitz, J. Schmalstieg, H. Blanke, A. Warnecke, and D. U. Sauer, "Calendar and cycle life study of Li (NiMnCo) O₂-based 18650 lithium-ion batteries," *Journal of Power Sources*, vol. 248, pp. 839–851, 2014.
- [15] V. Srinivasan and J. Newman, "Existence of path-dependence in the LiFePO₄ electrode," *Electrochemical and Solid State Letters*, vol. 9, no. 3, p. A110, 2006.
- [16] A. Li, S. Pelissier, P. Venet, and P. Gyan, "Fast characterization method for modeling battery relaxation voltage," *Batteries*, vol. 2, no. 2, p. 7, 2016.
- [17] A. Barai, G. H. Chouchelamane, Y. Guo, A. McGordon, and P. Jennings, "A study on the impact of lithium-ion cell relaxation on electrochemical impedance spectroscopy," *Journal of Power Sources*, vol. 280, pp. 74–80, 2015.
- [18] C. J. Wen, B. Boukamp, R. A. Huggins, and W. Weppner, "Thermodynamic and mass transport properties of "LiAl"," *Journal of The Electrochemical Society*, vol. 126, no. 12, p. 2258, 1979.
- [19] Y. Zhu, T. Gao, X. Fan, F. Han, and C. Wang, "Electrochemical techniques for intercalation electrode materials in rechargeable batteries," *Accounts of chemical research*, vol. 50, no. 4, pp. 1022–1031, 2017.
- [20] D. W. Dees, S. Kawauchi, D. P. Abraham, and J. Prakash, "Analysis of the galvanostatic intermittent titration technique (GITT) as applied to a lithium-ion porous electrode," *Journal of Power Sources*, vol. 189, no. 1, pp. 263–268, 2009.
- [21] W. Waag, S. Käbitz, and D. U. Sauer, "Experimental investigation of the lithium-ion battery impedance characteristic at various conditions and aging states and its influence on the application," *Applied energy*, vol. 102, pp. 885–897, 2013.
- [22] Y. Zhang, C.-Y. Wang, and X. Tang, "Cycling degradation of an automotive LiFePO₄ lithium-ion battery," *Journal of power sources*, vol. 196, no. 3, pp. 1513–1520, 2011.
- [23] M. Ecker, J. B. Gerschler, J. Vogel, S. Käbitz, F. Hust, P. Dechent, and D. U. Sauer, "Development of a lifetime prediction model for lithium-ion batteries based on extended accelerated aging test data," *Journal of Power Sources*, vol. 215, pp. 248–257, 2012.
- [24] J. Taylor, A. Barai, T. Ashwin, Y. Guo, M. Amor-Segan, and J. Marco, "An insight into the errors and uncertainty of the lithium-ion battery characterisation experiments," *Journal of Energy Storage*, vol. 24, p. 100761, 2019.
- [25] M. J. Lacey, "Influence of the electrolyte on the internal resistance of lithium- sulfur batteries studied with an intermittent current interruption method," *ChemElectroChem*, vol. 4, no. 8, pp. 1997–2004, 2017.
- [26] B. Aktekin, M. J. Lacey, T. Nordh, R. Younesi, C. Tengstedt, W. Zipprich, D. Brandell, and K. Edström, "Understanding the capacity loss in LiNi_{0.5}Mn_{1.5}O₄-Li₄Ti₅O₁₂ lithium-ion cells at ambient and elevated temperatures," *The Journal of Physical Chemistry C*, vol. 122, no. 21, pp. 11 234–11 248, 2018.
- [27] A. Bergfelt, M. J. Lacey, J. Hedman, C. Sångeland, D. Brandell, and T. Bowden, "ε-caprolactone-based solid polymer electrolytes for lithium-ion batteries: synthesis, electrochemical characterization and mechanical stabilization by block copolymerization," *RSC advances*, vol. 8, no. 30, pp. 16716–16725, 2018.
- [28] A. Bergfelt, G. Hernández, R. Mogensen, M. J. Lacey, J. Mindemark, D. Brandell, and T. M. Bowden, "Mechanically robust yet highly conductive diblock copolymer solid polymer electrolyte for ambient temperature battery applications," *ACS Applied Polymer Materials*, vol. 2, no. 2, pp. 939–948, 2020.
- [29] R. Mogensen, S. Colbin, and R. Younesi, "An attempt to formulate non-carbonate electrolytes for sodium-ion batteries," *Batteries & Supercaps*.
- [30] Y.-C. Chien, A. S. Menon, W. R. Brant, D. Brandell, and M. J. Lacey, "Simultaneous monitoring of crystalline active materials and resistance evolution in lithium-sulfur batteries," *Journal of the American Chemical Society*, vol. 142, no. 3, pp. 1449–1456, 2019.
- [31] M. Kim and E. Hwang, "Monitoring the battery status for photovoltaic systems," *Journal of power sources*, vol. 64, no. 1-2, pp. 193–196, 1997.
- [32] M. Dubarry, C. Truchot, B. Y. Liaw, K. Gering, S. Sazhin, D. Jamison, and C. Michelbacher, "Evaluation of commercial lithium-ion cells based on composite positive electrode for plug-in hybrid electric vehicle applications. part I: Initial characterizations," *Journal of power sources*, vol. 196, no. 23, pp. 10 328–10 335, 2011.
- [33] Z. Geng, T. Thiringer, Y. Olofsson, J. Groot, and M. West, "On-board impedance diagnostics method of Li-ion traction batteries using pseudo-random binary sequences," in *2018 20th European Conference on Power Electronics and Applications (EPE'18 ECCE Europe)*. IEEE, 2018, pp. P-1.
- [34] U. K. Kalla, R. Suthar, B. Singh, K. Sharma, and J. Singhal, "Generalized electronic controller for multi-pulse battery charging systems," in *2016 IEEE 6th International Conference on Power Systems (ICPS)*. IEEE, 2016, pp. 1–6.
- [35] M. Bayati, M. Abedi, M. Farahmandrad, and G. B. Gharehpetian, "Delivering smooth power to pulse-current battery chargers: Electric vehicles as a case in point," *IEEE Transactions on Power Electronics*, vol. 36, no. 2, pp. 1295–1302, 2020.
- [36] S. S. Sebastian, B. Dong, T. Zerrin, P. A. Pena, A. S. Akhavi, Y. Li, C. S. Ozkan, and M. Ozkan, "Adaptive fast charging methodology for commercial Li-ion batteries based on the internal resistance spectrum," *Energy Storage*, vol. 2, no. 4, p. e141, 2020.
- [37] C. Lazaroïu, G. C. Lazaroïu, M. Pagano, and M. Roscia, "Smart agent to optimize recharge of electric vehicles (evs) into smart cities," in *2018 International Symposium on Power Electronics, Electrical Drives, Automation and Motion (SPEEDAM)*, 2018, pp. 437–442.
- [38] J. Li, E. Murphy, J. Winnick, and P. A. Kohl, "The effects of pulse charging on cycling characteristics of commercial lithium-ion batteries," *Journal of Power Sources*, vol. 102, no. 1-2, pp. 302–309, 2001.
- [39] H. A. Serhan and E. M. Ahmed, "Effect of the different charging techniques on battery life-time," in *2018 International Conference on Innovative Trends in Computer Engineering (ITCE)*. IEEE, 2018, pp. 421–426.



Zeyang Geng Zeyang Geng is a PhD student at Chalmers University of Technology working with characterization, modelling and aging of lithium ion batteries. She took her B.Sc at Zhejiang University in 2013 and M.Sc at Chalmers University of Technology in 2015.



Torbjörn Thiringer Torbjörn Thiringer works at Chalmers University of Technology, in Göteborg Sweden, as a professor in applied power electronics. He took his M.Sc and Ph.D at Chalmers University of Technology in 1989 and 1996 respectively. His areas of interest include the modeling, control and grid integration of wind energy converters into power grids, battery technology from cell modelling to system aspects, as well as power electronics and drives for other types of applications, such as electrified vehicles, buildings and industrial applications.



Matthew J. Lacey Matthew Lacey received his MChem and PhD degrees from the University of Southampton in 2008 and 2012, respectively, with a focus on electrochemistry and new materials for lithium-ion batteries. He joined Uppsala University in 2012 to focus on lithium-sulfur battery chemistry, and in 2019 joined Scania CV AB as a Development Engineer in Materials Technology, with a focus on battery cell analytics, electrochemical methods and next-generation battery chemistries.